Report on Damage to Infrastructures by the Mid Niigata Prefecture Earthquake in 2004

by

NILIM-PWRI Joint Reconnaissance Team for the Mid Niigata Prefecture Earthquake in 2004

ABSTRACT

The October 23, 2004 Mid Niigata Prefecture earthquake of magnitude 6.8 in JMA scale and the subsequent aftershocks, which struck the inland area of Niigata prefecture, was the most severe earthquake to affect Japan since the 1995 Hyogo-ken Nambu earthquake. The earthquake resulted in 46 deaths and three thousand injuries. It also destroyed over 90,000 houses.

A reconnaissance survey was conducted under the cooperation of NILIM and PWRI to observe, document and summarize the damage and learn lessons from this earthquake that can be used to mitigate the impact of future earthquakes.

This paper briefly summarizes the information collected during as well as following this investigation. The paper includes information on geology, landslides, damage to road facilities and sewerage systems. Other lifeline systems and buildings were out of scope of the survey. Damage to dams is not described as they are to be reported in a separate paper.

KEYWORDS: Earthquake damage, 2004 Mid Niigata Prefecture Earthquake

1. SUMMARY OF THE EARTHQUAKE

1.1. Hypocenter and seismic intensity distribution

The 2004 Mid Niigata Earthquake occurred at 5:56 pm on October 23, 2004. The hypocenter was located at 37.288° N, 138.87° E. The rupture started at a depth of 13km and produced an earthquake with JMA magnitude of 6.8 [1]. Distribution of JMA seismic intensity and the epicentre location, together with the surface projection of an approximate fault plane are plotted in Fig. 1 [2]. The maximum seismic intensity of the earthquake was 7 and measured at Kawaguchi. The seismic intensities measured at the other stations were: 6+ at Ojiya, Yamakoshi and Oguni, 6- at Nagaoka, Tokamachi, Tochio and the other nine stations.

The major disaster area, such as Kawaguchi and Yamakoshi, was located just above the fault plane. The focal mechanism of this earthquake is the reverse fault type with a strike of approximately N35E. This type of inland earthquake with a magnitude larger than or equal to 6.8 occurred after an absence of 60 years (previous one is the 1945 Mikawa Earthquake, M=6.8). In this period, there were six strike-slip fault type earthquakes with magnitudes larger than or equal to 6.8. It should be noted that the number of large aftershocks of this earthquake is significantly greater than the other recent inland earthquakes in Japan (two aftershocks with a maximum seismic intensity of 6+, two 6-, eight 5+, six 5-).

1.2. Characteristics of the earthquake motion

Ministry of Land, Infrastructure and Transport maintains strong-motion seismograph network deployed all over Japan for infrastructure maintenance. The earthquake motions were observed at about 180 stations in this network during the earthquake. Peak ground accelerations observed by the network are shown in Fig. 2. The observed peak accelerations and calculated spectral intensities can be obtained at the National Institute for Land and Infrastructure Management Website [3]. The maximum acceleration observed in the network was 1715cm/s^2 at MYK (located 7km northeast of the epicentre). The maximum spectral intensity, considered a good index to damage to structures, was also observed at MYK (106cm/s in EW-direction). This maximum value is comparable to that observed at the JMA Kobe Marine Observatory during the 1995 Hyogo-ken Nambu (Kobe) Earthquake (114cm/s in NS-direction).

1.3. Acceleration records and response spectra

Observed acceleration records at MYK and NGK are shown in Fig. 3. Calculated JMA seismic intensities at these stations are 7 and 6+, respectively. Observed peak accelerations and spectral intensities also suggest that earthquake motions at these sites were very strong. Response spectra of these stations are shown in Fig. 4, together with that obtained from the record at the JMA Kobe Marine

Observatory in the 1995 Hyogo-ken Nambu Earthquake. We can see that the earthquake motion observed at MYK is as strong as that observed at the JMA Kobe in general and stronger for structures with short natural period.

2. TOPOGRAPHY AND GEOLOGY

2.1. Hills

Geological map of the Mid Niigata is shown in Fig. 5. The major epicentres of the earthquake are centred on the hills at an altitude from 10 to 100m.

Feature of topography in this area is characterized by rivers and ridge of hill extended from north-northeast to south-southwest (Fig. 6). Ridgelines of main hills and the bottom plain of valley almost correspond to synclinal axis and anticlinal axis respectively. This was due to crustal movement from Pleistocene to the recent.

This area is well known to be one of major landslide areas in Japan. Sedimentary rocks after the Neocene with composite fold systems are distributed thickly. They are classified to soft rocks in engineering, and are intercalated by unconsolidated mudstone and tuff layers, which caused landslides in this earthquake.

2.2. Terraces

Many fluvial terraces have been developed along the river in this area. Especially current researches divided these terrace surfaces into about ten stages along the Shinano River. However surface of terraces were originally flat, some of them were deformed by active faults and flexures. The old terraces are deformed largely than new ones. Additionally, geodetic studies have shown that this area has undergone a rise and a fall in elevation at a rate from 0.1 to 1 mm/y between Pleistocene and the recent.

2.3. Basins, Plains and Rivers

The source region has the Shinano River and its sub rivers. Tokamachi Basin in the upper Shinano River in the west of the source region has few alluvial plains as scarps of terrace are close to present streams. And Muikamachi Basin in the upper Uonogawa River in the south is composed of thick gravel layer that is widely overlain by alluvial fan sediment. Therefore, the sand layer leading to liquefaction is more widely distributed in Niigata alluvial plain than one around Ojiya City.

2.4. Active fault

Distribution of active faults in this area is shown in Fig. 6. Most of faults are reverse faults and accord with terrain and geological structure. The hill and the plain correspond to the hanging wall and the foot wall respectively along faults.

The earthquakes were centred at Obiro Fault and nearby concealed active faults in the subsurface. However, the rupture and displacement are considered not to reach to the ground surface in this earthquake.

3. SUMMARY OF DAMAGE

3.1. Numbers of casualties and damaged residential houses

Table 1 summarises numbers of casualties and damaged residential houses in the earthquake (as of 9:00 March 18, 2005). Forty fatalities have resulted from the earthquake; 16 of these from collapse of buildings (direct losses) and the rest due to shock of the earthquake or post-earthquake stress. Number of house losses caused by fire was limited even though the earthquake occurred just before dinner-time (6:00 pm).

3.2. Landslides and slope failures

The damaged area is a hilly mountainous area underlain by young, weak sedimentary rocks formed in the tertiary period. The landslide hazards have been very widely distributed in the area, and many slope failures, landslides and debris flow occurred in the earthquake. 3791 slope failure sites were identified by aerial photographic surveying. Rate of slope failure incidence was very high compared to those in the past earthquakes.

Slope failures and landslides formed several new lakes by damming the Imo River, a tributary of the Uono River, and level rising in a lake inundated the upstream village. These lakes posed downstream hazards because of the possible failure of their natural dams, which could have resulted in catastrophic downstream flooding.

3.3. Public sewerage system

Damage to the sewerage pipeline system was widely distributed in the Mid Niigata area. Uplifting of pipes and manholes due to subsoil liquefaction, breakage and blocking up of pipes, relative horizontal displacements of manhole assembled blocks, breakage of pipe joints were observed. Some of the manholes were lifted up by more than 1m.

Damage was also found at twelve sewage-treatment plants and twelve pumping stations. In Horinouchi Plant, cracking in a water treatment plant and tilting of a sludge thickener resulted in malfunction of sewerage processing.

3.4. River and related facilities

Major damage found was cracking of river dykes and quay walls. Some of the river dykes showed subsidence and failures. Damage also observed in some sluiceways and weirs. In upstream of Ojiya, damage found was not so severe although number of damaged sites was relatively large. In downstream of Ojiya, damage was relatively severe although number of damaged sites was small. In Myoken Weir where peak acceleration exceeding $15m/s^2$ was observed, covering concrete peeled off a concrete gatepost resulting in exposure of main reinforcements.

3.5. Dams and pondages

Inspection of 114 dams and pondages was made just after the earthquake and revealed that only three irrigation dams at Ojiya, Tokamachi and Kawanishi and three dams for hydraulic power generation station of Japan Railway East showed some deformations. Cracking in crest and inward settlement of dam body were observed. In the Asagawara regulating pondage that was most severely damaged fill-type dam, longitudinal cracking occurred along the crest and the upstream slope settled down.

3.6. Road and related facilities

Three road bridges in Nagaoka and Ojiya were damaged. In these bridges, damage was found at (1) portions where area of main reinforcement was changed in reinforced concrete piers, (2) shoes, and (3) beam ends and abutment parapets between which smashing against each other occurred. Subsidence of abutment backfill was also observed. Types of damage observed in the earthquake are similar to those in the past earthquakes.

Number of closure sites in national and local roads due to damage in earthworks and slope failures was 209. Probably heavy rainfall brought by Typhoon No.23 three days before the earthquake made water content of soils higher, resulting in large number of earthwork failures. Damage found in earthworks was; (1) slope failure of embankments, (2) overturning of concrete block retaining walls, (3) settlement of box culverts underpassing expressway embankment and opening of their joints, and (4) cut slope failures.

Ten road tunnels were damaged. Severe damage was found in Wanatsu Tunnel on Route No.17, such as, falling of concrete lining from the tunnel crown, inward movement of side walls, compression failure of the concrete lining at springline, and deformation of a lateral groove.

4. LANDSLIDES

4.1. Overview

Landslides occurred at many locations in mountain slopes. Distribution of landslides together with epicentres of main shock and two of aftershocks are shown in Fig. 7 (indicated by gray areas). The figure shows that the landslides are concentrated in the area near the main shock epicentre. According to the analysis of satellite and aerial photographs covering the most affected area including Yamakoshi Village and the vicinity, 1662 slope failures were found and they covered 4.7 % of the whole area that is much larger than the case of the 1995 Kobe earthquake (0.2 %). The most affected area is characterized as that many landslide sites of tertiary strata have been distributed. It should be also noted that there were precipitation of 448 mm in the last one month before the earthquake. The prior rainfall might have caused to increase the number of landslide occurrence during the earthquake.

The most notable consequence of the landslides due to the earthquake was that several landslide dams were formed in Imo River that run through Yamakoshi Village.

4.2. Landslide Dams and Emergency Response

Locations of landslide dams that were formed in Imo River by the earthquake are indicated in Fig. 8. Dimensions and volume of the landslide dams are presented in

Table 2. The landslide dams dammed up the river and created dam lakes. As a result, some of the upstream villages were inundated and the village people were forced to evacuate to Nagaoka City. The dams also threaten the downstream area. Once they break, large mud and debris flows attack downstream area. The dams breaking may be triggered by overflow or piping.

Risk assessment of the dams breaking was made based on the empirical data and formulae, and the results obtained from the assessment were:

1) Time required to cause overflow is much shorter than that for piping.
2) Two large landslide dams at Terano and Higashi-Takezawa have potential to be eroded out by overflow. (Fig. 9 was used for the assess-

ment. The threshold line to judge the potential of overflow-induced erosion was developed with past case records.)

3) Once the dams are eroded out, there is a very high risk of large mud and debris flows attacking the downstream Ryuko District.

It was concluded from the results of the assessment that any possible emergency response to prevent overflow should be taken as early as possible. In order to draw down the dam lake elevation, drainage by pumping was taken as the first step. Then, drainage channels were constructed by excavating the landslide dams. They were completed within the start of snow season, and the dam lakes elevation has been kept low.

4.3. Landslide at Higashi-Takezawa District

Photo 1 shows the landslide at Higadshi-Takezawa. Dimensions of the sliding block were 295 m wide and 350 m long in slope direction. The sliding distance was about 100 m, and the soil mass collided the opposite slope. No sliding occurred at the opposite slope.

It is observed in the topographic map before the earthquake (Fig. 10, together with plan view of the landslide) that the slope inclination of the landslide is mild less than 20 degrees while that of the opposite slope is much steeper. This contrast is associated with the fact that the landslide slope was a dip slope and the opposite slope was a reverse dip.

The sliding mass consisted mainly of brown-coloured sandy soil, and the bedrock was blue-grey siltstone. Grain-size distributions of the sliding mass are presented in Fig. 11. This shows that the sand contents (D=0.075 - 2.0 mm) of the two samples for this site are 70 to 80 %.

Slope inclination of outcropped sliding surface was about 20 degrees. Also, the upside slope that was stable during the earthquake had the almost same inclination. In addition, it was observed in the topographic map before the earthquake that there existed slight dips along the perimeter of the sliding mass. These evidences suggest that the landslide was the secondary landslide.

4.4. Landslide at Terano District

Photo 2, Fig. 12 and Fig. 13 show the landslide at Terano District. Dimensions of the sliding mass were 230 m wide and 360 m long in slope direction. The sliding mass formed a landslide dam and clogged the river flow. Similar to the case at Higashi-Takezawa, the landslide slope was a dip slope.

The sliding mass consisted mainly of brown-coloured sandy soil, and the bedrock was mudstone. A soil sample taken from the sliding mass had a sand content of 90 % (see Fig. 11). The sliding mass consisted of three sub-blocks as indicated in Fig. 12 and Fig. 13. By comparing with the topographic map drawn before the earthquake, this slide was presumed to be the secondary landslide. Many cracks and gaps were formed on the surface of sliding masses. Infiltration of rain and snow melting water from theses cracks and gaps might cause further movement of the sliding masses. Therefore, an emergency response was required to prevent the secondary disaster due to the movement.

5. SEWERAGE SYSTEMS

5.1. Summary of damage

Damage to the sewage systems due to the earthquake is widely distributed in the Mid Niigata area. The damage was observed in 26 cities, towns and villages, and 37 sewage systems. The damaged sites were totally counted more than 13,000. More than twenty-percent of sewers was damaged in Ojiya City, Kawaguchi town and Oguni Town near the epicentre of the earthquake. Damage was also found at twelve sewage-treatment plants and twelve pumping stations. In Horinouchi Plant, cracking in a water treatment tank and tilting of a sludge thickener resulted in malfunction of sewerage processing.

5.2. Typical damage types and mechanisms

Two typical damage types were showed in Photo 3 and Photo 4. The damage of road pavements along backfills of sewers and manholes was found at about 6000 sites. The uplift of manholes was observed at about 1500 sites. The maximum uplift displacement was more than 1m. Similar damage was observed in the 2003 Tochachi-oki Earthquake and the 1993 Kushiro-oki Earthquake, the 1993 Hokkaido Nansei-oki Earthquake. These damaged sites were chiefly distributed in the area where soft clay or peat layer exists. Recent research results indicate that backfill at the damaged sites was liquefied due to the following factors:

- Groundwater level was high, and backfill was widely saturated.
- Backfill was loosened when earth retaining sheet piles used for excavation were removed

after finishing back filling.

- Backfill was subjected to cyclic shearing during earthquake under almost undrained condition, since excess pore water pressure built by cyclic shearing in the backfill could not dissipate to the surrounding low permeability original ground.

Identified mechanisms of typical damage due to liquefaction are illustrated in Fig. 14.

5.3. Emergency technical proposals for full restoration of damaged sewerage pipelines

The Technical Committee for the Restoration of Earthquake Damage to the Sewerage Systems consisting of academic experts was established after the earthquake. The committee proposed three backfilling methods tabulated in Table 3 for the full restoration. Improvements of the backfill are the most effective measures, because most of the damage is caused by the backfill liquefaction. Compaction of the backfill increases liquefaction resistance and decrease uplift displacement of sewer and manhole. Backfill with crushed stone has high water permeability and resists liquefaction. Backfill consisting of cement mixed sand also resists liquefaction strongly.

6. ROAD AND RELATED FACILITIES

Roads and highways in the affected area were severely damaged. In particular, damage-induced closing of Kan-etsu Expressway and National Road Route No. 17 that connect Tokyo with the area and the northern part affected very much to transportation. Failures of earth structures were found at many locations, and buckling of bridge piers and distortion of tunnels were observed at several locations. In spite of damage and closing of the roads in the area, the other road network compensated the traffics and transportation during the period until temporary restoration was completed.

6.1. Road bridges

Damage was found at (1) portions where area of main reinforcement was changed in reinforced concrete piers, (2) shoes, and (3) beam ends and abutment parapets between which smashing against each other occurred. Subsidence of abutment backfill was also observed. Types of damage observed in the earthquake are similar to those in the past earthquakes. Details of damage in Shinkumi Overpass, Ojiya and Yamanobe Bridges are described in the following subsections.

6.1.1. Shinkumi Overpass (Shinkumi-cho, Nagaoka City)

Route No. 8 passes over JR Shin'etsu Line. Construction of the overpass was completed in 1989. The superstructure consists of a two-span continuous steel plate girder bridge, three simple steel plate girder bridges, and a two-span continuous steel plate girder bridge. These are supported by cylindrical reinforced concrete piers on pile foundations through bearings with bearing plates.

In pier No.5, (1) covering concrete falling off, (2) buckling of main reinforcements, and (3) breakage of main reinforcement lap joints were observed at the point where area of main reinforcement was changed (Photo 5). In pier No.6, diagonal shear cracks and gapping between the covering and reinforcement were found. In the other piers, diagonal and horizontal shear cracks were observed at the top of concrete column. Five upper parts of the shoes on abutment No.2 on down line showed damage in devices that limit excessive displacement. The most severe damage in the shoes was found in those supporting outermost girders.

6.1.2. Ojiya Bridge (Ojiya City)

Ojiya Bridge in Route No. 17 crosses over Shinano River. Construction of the bridge was completed in 1982. The superstructure consists of a four-span continuous box girder bridge and a three-span continuous box girder bridge. These are supported by cylindrical reinforced concrete piers on pile foundations through hinged and roller bearings. In the pier supporting the four-span bridge through the hinged bearings, (1) covering concrete falling off, (2) buckling of main reinforcements, (3) breakage of main reinforcement lap joints, and (4) diagonal shear cracks were observed at the top of RC column. Three piers supporting the bridge through the roller bearings showed diagonal and horizontal shear cracks on the upstream side. The other damage found were; (1) breakage of devices limiting excessive displacement for the upper part of the shoe, (2) breakage of side blocks for the lower parts of the shoe (Photo 6), (3) deformation of a bottom flange of the three-span continuous box girder bridge around the hinged bearing, and (4) local buckling and cracks in a stiffener on the shoe.

6.1.3. Yamanobe Bridge (Yamanobe-cho, Ojiya City)

Yamanobe Bridge in Route No. 117 passes over conducting tubes of JR East Shinano river power station. Construction of the bridge was completed in 1986. The superstructure consists of a simple steel I-girder bridge, a steel Lohse bridge, a simple steel box-girder bridge, and two simple steel I-girder bridges. These are supported by a RC wall type pier, a RC rigid frame pier, a two-story RC rigid frame pier with circular columns, and a RC rigid frame pier with circular columns. Foundation of the substructure was made by Shinso method (a kind of large diameter cast-in-place piles). The shoes for simple girder bridges are the bearing with bearing plates and those for the Lohse bridge are hinged and roller bearings.

In the pier supporting the Lohse bridge through the hinged bearing, (1) falling-off of covering concrete, (2) buckling of main reinforcements, (3) breakage of tie hoop lap joints were observed. In the two-story RC rigid frame pier with circular columns, the following damage was found; (1) vertical cracks in the upper beam near the mountain-side column, (2) shear cracks parallel to the slope in the middle of the mountain-side column, (3) cracks propagating from the upslope to the down-slope in the lower beam. In the mountain-side column of the pier located between two simple steel I-girder bridges (RC rigid frame pier with circular columns), cracks propagating from the bottom to the middle of the column were observed. Apart from the damage mentioned above, breakage of devices limiting excessive displacement for the upper part of the shoe and exposure of the pile heads due to ground surface subsidence were found.

6.2. Road Embankments and Slopes

6.2.1. Overview

Sites where road embankments or slopes were damaged and the traffics were closed are plotted in Fig. 15. Of a total of 241 closed sites on the national and prefectural roads, 209 sites were associated with damage to embankments or slopes. There was a considerable amount of precipitation in the last five days before the earthquake in the area. In Nagaoka, it was 124 mm. It is considered that that the rainfall caused the soils wet and thus increased the amount and extent of damage to the earth structures and slopes. Some of the typical damage are briefly described in the following.

6.2.2. Flow sliding of embankment slopes

Photo 7 shows sliding failure of the embankment slope at kilopost 215.1 of Kan-etsu Expressway. The road segment was cut-and-bank (a cut slope on the left-hand side of the photo, and embankment slope on the right-hand side). The failed soil block corresponds to the fill material. It was observed that the soil at the bottom of the failed soil was very wet and almost saturated. Therefore, it is presumed that the bottom part of the fill was saturated with seepage water at the time of earthquake, and the soil was liquefied to have induced sliding failure.

Photo 8 shows sliding failure of the embankment slope at Hosojima of Route No.117. The site conditions and the type of failure are very much similar to the above-mentioned case. Photo 6.3 also shows that the failed soil travelled far away from the embankment toe to the paddy field. The soil was also highly saturated. These evidences indicate that the failure was the flow slide that was induced by liquefaction of fill soils.

6.2.3. Failure of embankment slope on steep base rock

Photo 9 shows the sliding failure at Ten-noh, Route No. 17. An aerial picture of the same site is also shown in Photo 10. The road and railway run along the edge of river terrace of Shinano River. The river runs in the right-hand side of Photo 9 and Photo 10, and the height of the terrace relative to the riverbed is about 40 meters. The average inclination of the terrace slope is about 25 degrees. As can be seen in Photo 6.3, road fill slope and the neighbouring railway fill slope are sliding down as a soil mass. The width of the failure was 56 meters measured at the road shoulder. The base of the sliding was alternation of tertiary sandstone and mudstone overlain by terrace sand gravel. Observation of the scarp immediately after the earthquake showed that the road fill soil composed of gravel and sand was rather dry. However, the bottom layer of the railway fill was wet. Original topography of the damaged site corresponded to a valley, which suggests that underground seepage water tend to accumulate. The mechanism of the failure has not been made clear, but the possible reasons are (1) inertial force acting on the fill on the steep slope caused loss of stability, or (2) the bottom saturated soil of the railway fill liquefied due to the earthquake, triggering slope failure associating with the upside road fill.

Restoration work was performed by using the geosynthetic reinforced soil method for the road and railway fills within the end of 2004. The cross section of the restoration work for the road fill is given in Fig. 16.

6.2.4. Settlement of embankments and associating displacement of box culverts

The Kan-etsu expressway between Ojiya and Nagaoka consists of embankment constructed on the alluvium. The foundation soil in the area is generally soft clay with relatively thin sand layer. There are many box culverts underpassing the embankment to connect rural roads. The embankment slumped about 20 to 50 cm, and level difference was formed on the pavement at many locations where the culverts exist, as shown in Photo 11. The settlement of the embankment associated with the lateral spread, i.e., the embankment moved outward. The culverts displaced outward probably with drag force from the embankment, and consequently the joints between segments of culverts opened. The opening amounted to 30 cm and the surrounding embankment soil spilled down into the culverts (see Photo 12). However, no crack was observed in the culverts.

6.2.5. Damage to retaining walls

Retaining walls were also damaged. Photo 13 shows damaged L-shaped concrete retaining walls that support toe of road embankment of Kan-etsu expressway. The retaining walls with a height of 1.2 meters rotated forward with about 30 degrees. Some retaining walls collapsed at the bottom of the vertical wall. The retaining walls were pre-cast and no seismic design was considered. It would be interesting to investigate a wide variety of damage ranging from small distortion to collapse of vertical wall that took place in close vicinity.

6.3. Road tunnel

Severe damage was found in Wanatsu Tunnel on Route No.17. The tunnel is 300m long and accommodates two-way road. It was constructed by the bottom drift method and construction was completed in 1965. Cross section of the tunnel is shown in Fig. 17. Plan view and longitudinal section of the tunnel with geological formation are drawn in Fig. 18. The tunnel mainly passes through silty sandstone.

Locations of crack in the tunnel lining are indicated by gray areas in the tunnel expansion plan (Fig. 19). Spalling of concrete lining from the tunnel crown was observed throughout the length of 100m from the Nagaoka-side portal and large mass of lining (2m wide and 20m long) fell off from the crown at a distance of 100m from the Nagaoka-side portal as shown in Photo 14. Inward movement of side walls, compression failure of the concrete lining at springline, and deformation of a lateral groove (Photo 15) were also observed. Outside the tunnel, slope deformation and overturning of a retaining wall were found just above the Nagaoka-side portal.

For temporary repair, (1) voids were filled with concrete, and (2) placement of steel supports and shotcrete was made. For permanent repair, the concrete lining was placed inside the temporal tunnel supports.

7. SUMMARY

Damage caused by the 2004 Mid Niigata Prefecture earthquake may be characterized as follows:

(1) Numerous natural slopes and artificial fills were damaged.
(2) Shinkansen (Bullet train) cars on service derailed for the first time in its history.
(3) Scarcely populated areas with many aged people were severely damaged.
(4) Highway networks functioned well as detour to the destructed area, and temporary repair works of trunk roads including Kan-etsu expressway and National Road Route No. 17 were accomplished very quickly.

The paper briefly described the landslides, damage to road facilities and wastewater systems caused by the earthquake. Post-earthquake studies of the damage are conducted by the both research institutes. It is expected that the results provide insights to mitigate damage in the future earthquakes.

REFERENCES

1. JMA website: http://www.jma.go.jp/
2. Website of Earthquake Research Institute, University of Tokyo: http://www.eri.u-tokyo.ac.jp/
3. http://www.nilim.go.jp/japanese/database/nwdb
4. Uemura, T. & Yamada T.: Geology in Japan, 4. Central Japan part I, Kyoritsu Shuppan, 1998 (in Japanese).
5. http://www.fdma.go.jp/detail/416.html
6. K. Namekata and K. Fujiu, M. Ishihara: Report on Damage to Sewerage Systems by the 2003 Off-shore Tokachi Earthquake, Water Korea, 2003.

Table 1: Number of casualties and damaged houses [5]

Prefecture	Casualties			Damaged houses			Fire
	Fatalities	Missing	Injured	Total collapse	Half collapse	Partial damage	
Niigata	46	0	4,791	2,827	12,746	100,453	9
Nagano	0	0	3	0	0	0	0
Saitama	0	0	1	0	0	0	0
Fukushima	0	0	0	0	0	1	0
Gunma	0	0	6	0	0	1,055	0
Total	46	0	4,801	2,827	12,746	101,509	9

Table 2: Dimensions and volume of landslide dams

District name	Dimensions of landslide dam				
	Length (m)	Height (m)	Width (m)	Volume of land-slide mass (m^3)	Pondage capacity (Volume of storage) (m^3)
Terano	360	26	230	107,800	428,900
Nanpei	220	8	345	11,700	20,200
Naranoki	190	9	240	44,500	9,100
Higashi-takezawa	350	28	295	1,272,300	3,273,100
Jyunidaira	125	9	95	23,300	25,200

Table 3: Emergency Technical Proposals for the Backfill Work in the Full Restoration

Backfilling method	Criteria of backfill materials	Criteria of restoration
Compaction of backfill	Use of good quality sand	Relative compaction of 90 % or higher (depending on the site condition).
Backfilling with crushed stone	Crushed stone with: Median particle size (D_{50}): larger than 10mm Effective particle size (D_{10}): larger than 1mm	Relative compaction of 90 % or higher
Solidification of backfill	Unconfined compression strength of cemented soil lies between 100 and 200kPa	Strength in the field lies between 50 and 100kPa

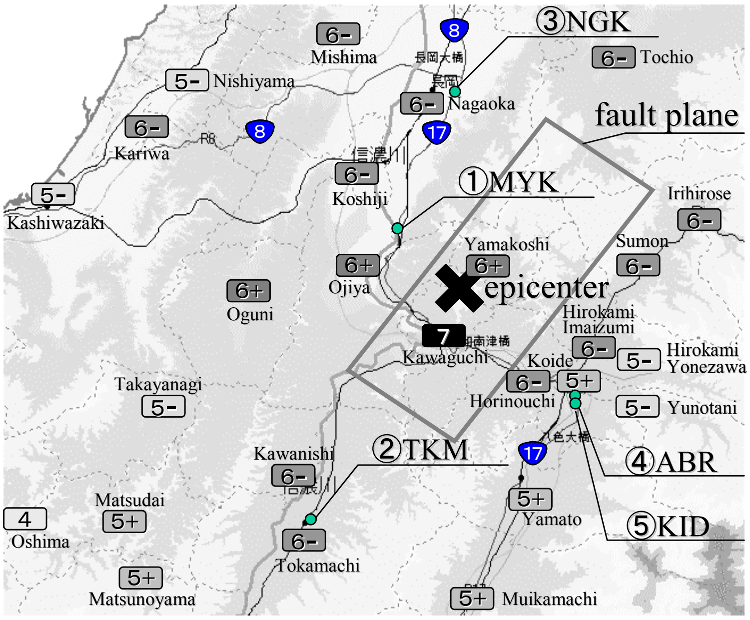

Fig. 1: Distribution of JMA seismic intensity and epicentre location

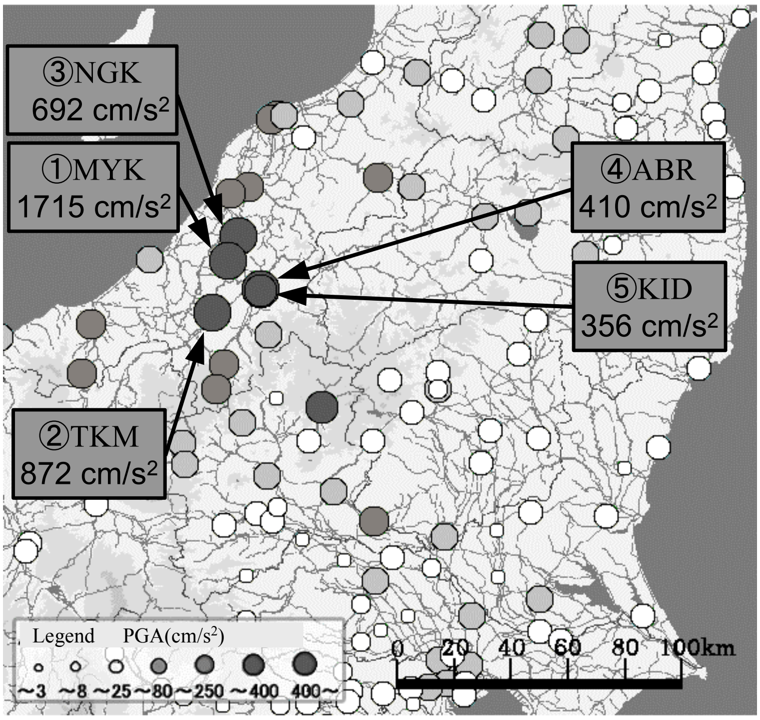

Fig. 2: Distribution of peak ground acceleration

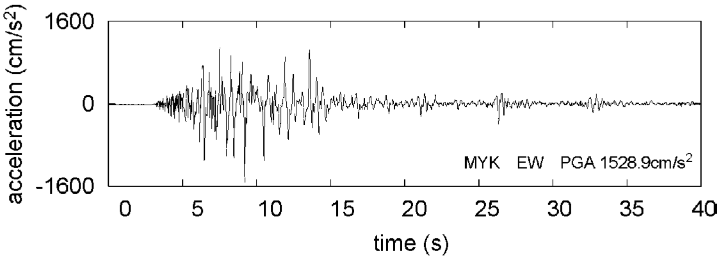

(a) MYK

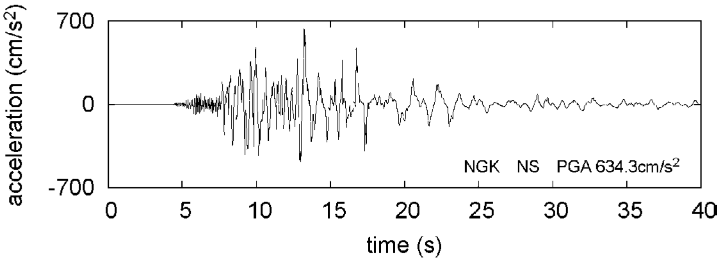

(b) NGK

Fig. 3: Acceleration waveforms observed at MYK and NGK

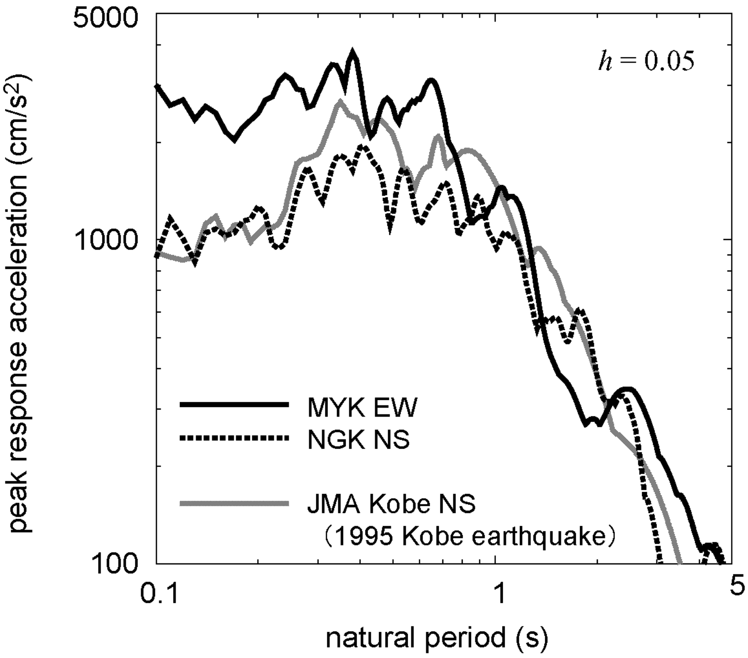

Fig. 4: Response spectra (damping ratio of 5%)

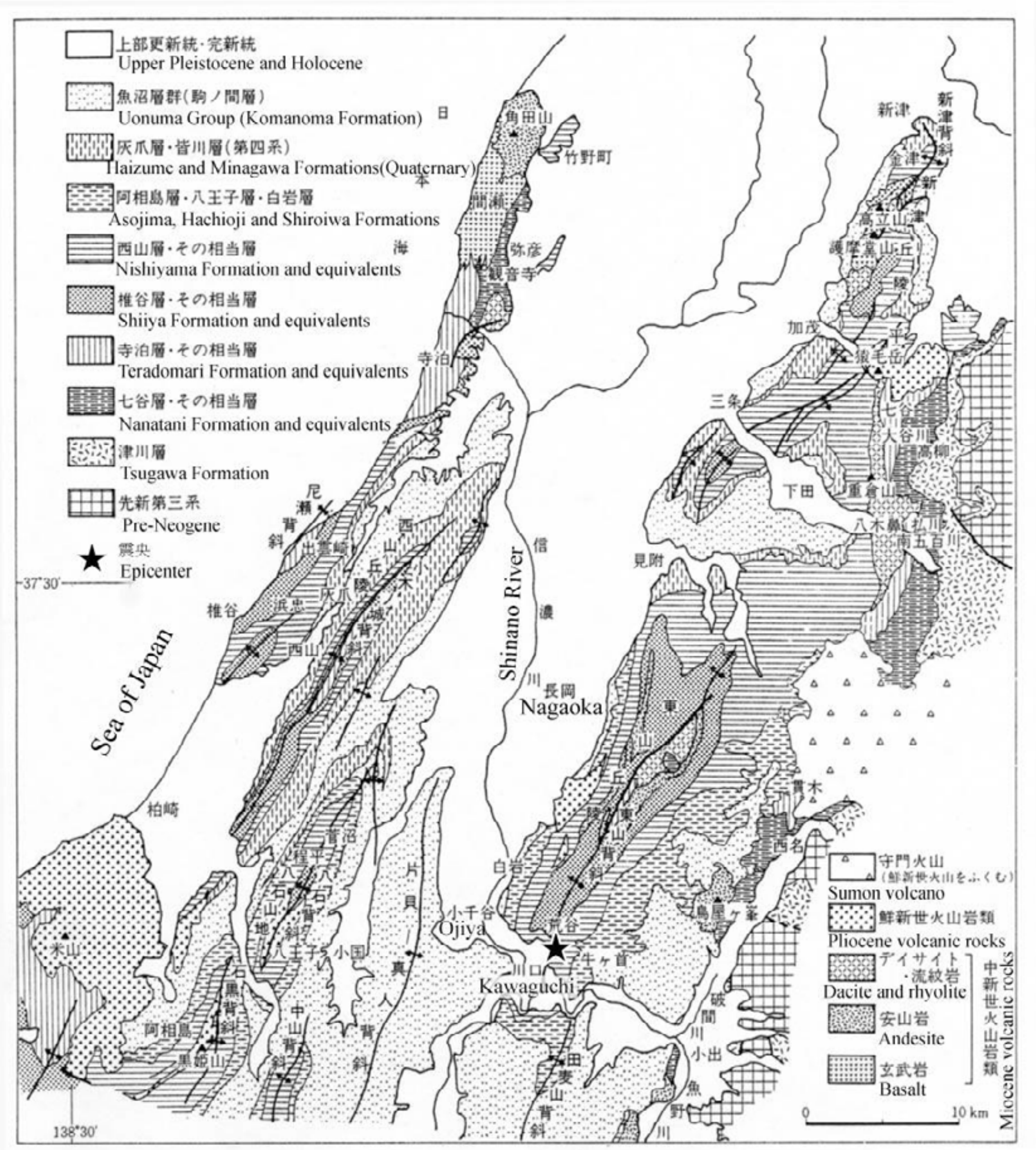

Fig. 5: Geological map of the Mid Niigata [4]

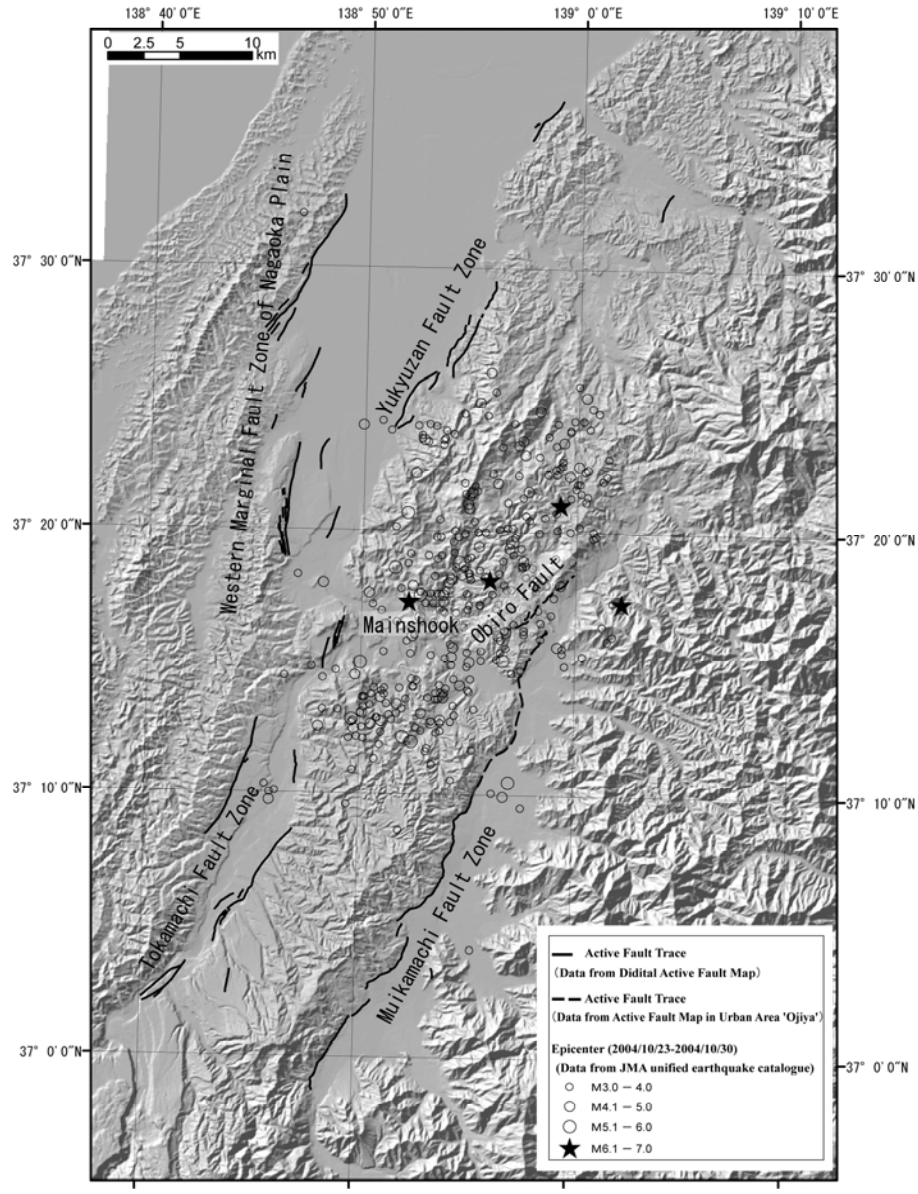

Fig. 6: Distribution of active faults (This map has used ‘Active Fault Shape File’ from Nakata,T. and Imaizumi, T., eds., 2002, “Digital Active Fault Map of Japan”, University of Tokyo Press (product serial number: DAFM0057). The background of this map has used Hillshade Map which was made from ‘Digital Map 50m Grid (Elevation)’ distributed by Geographical Survey Institute.)

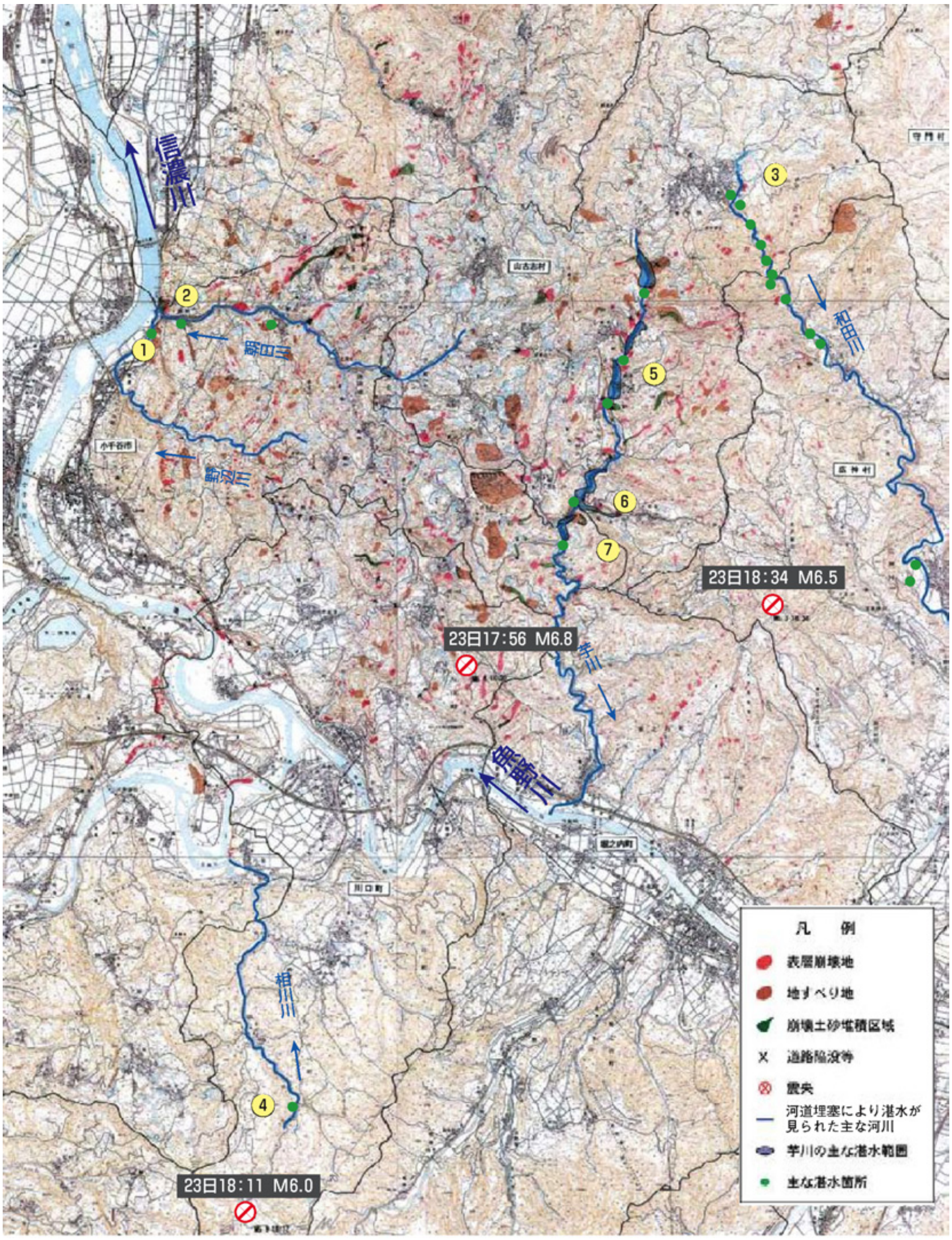

Fig. 7: Distribution of landslides and epicentre locations

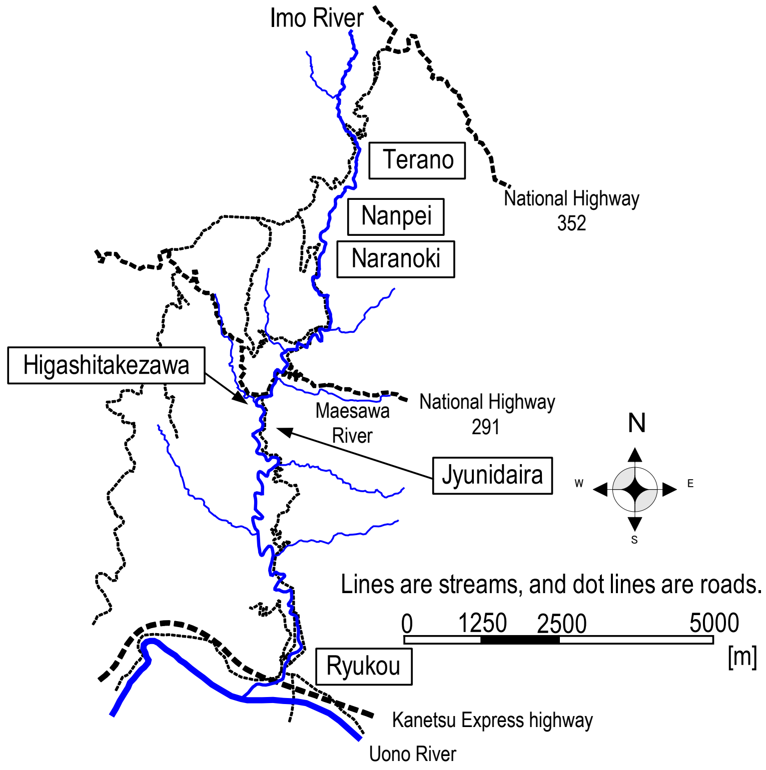

Fig. 8: Locations of landslide dams formed in Imokawa River

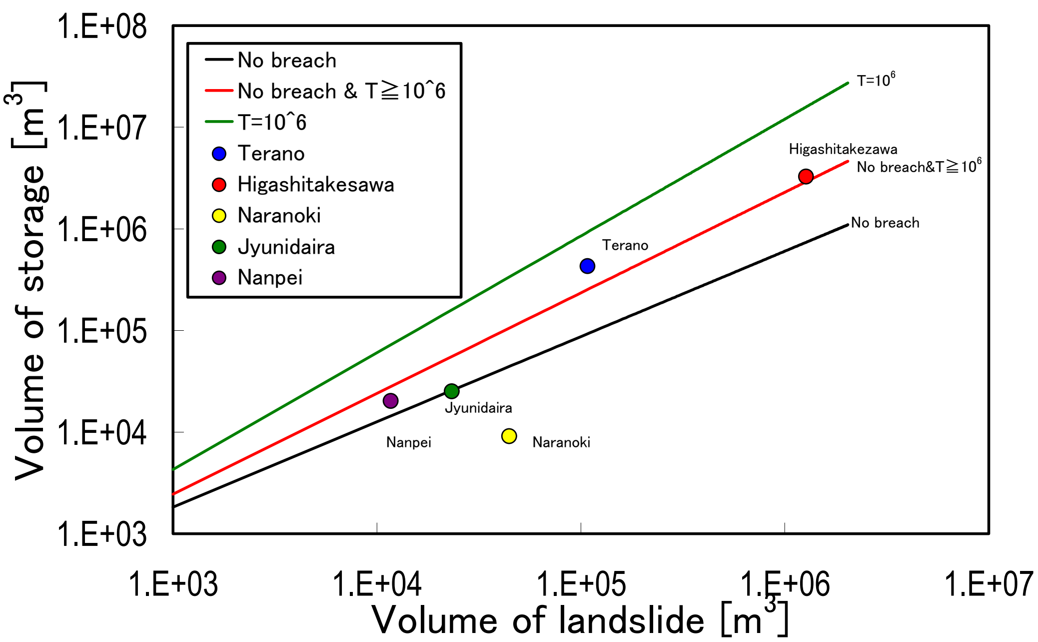

Fig. 9: Relationship between volume of landslide dam and impoundment

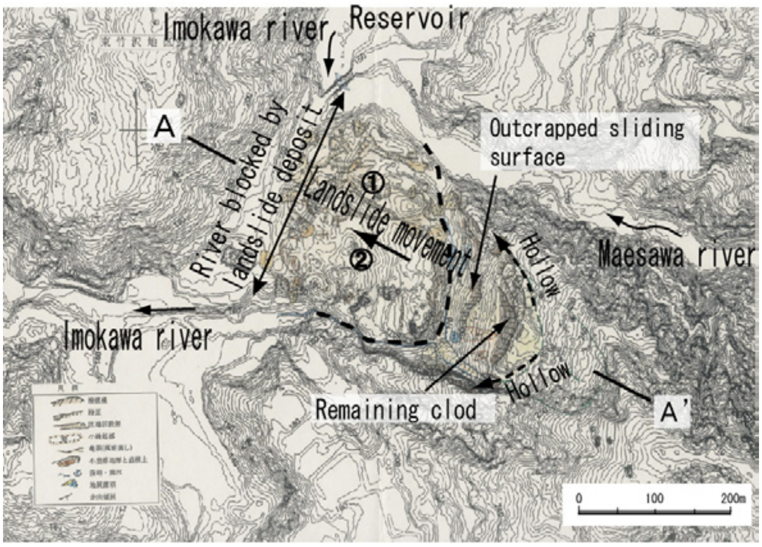

Fig. 10: Plan view of landslide at Higashi-Takezawa

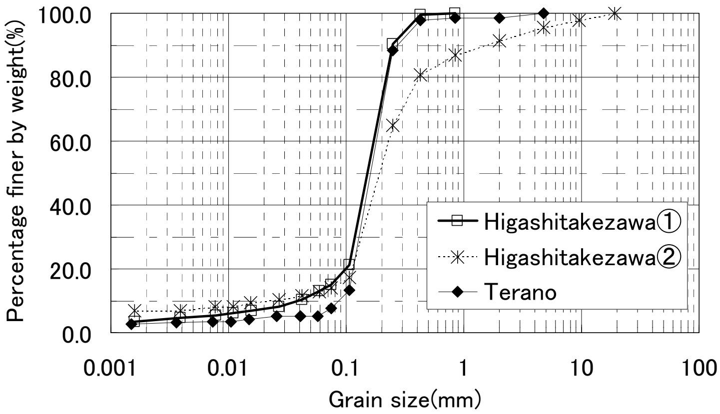

Fig. 11: Grain-size distributions of sliding mass

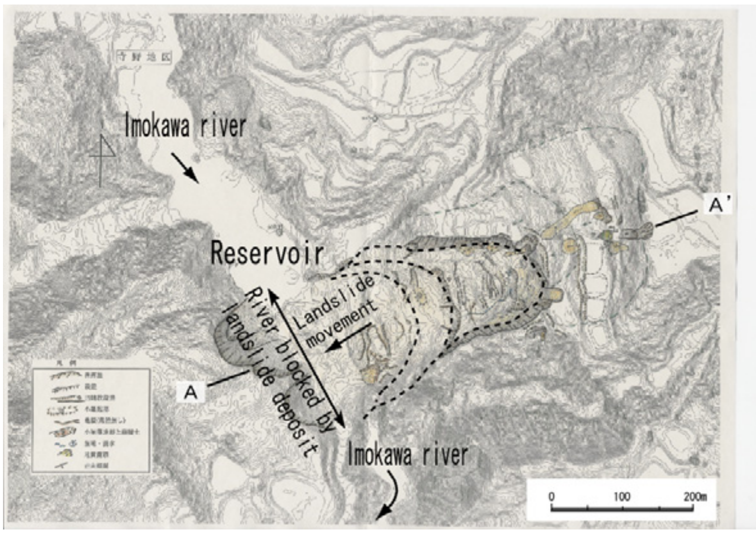

Fig. 12: Plan view of landslide at Terano

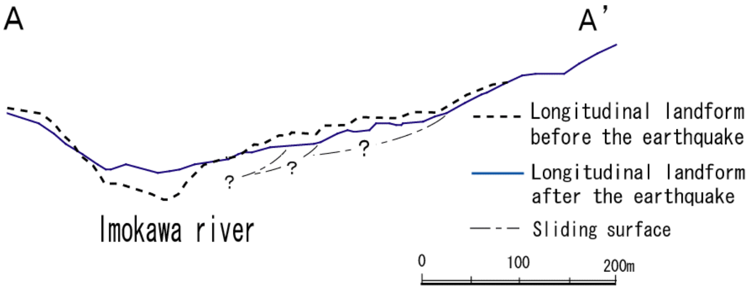

Fig. 13: Elevation of landslide at Terano

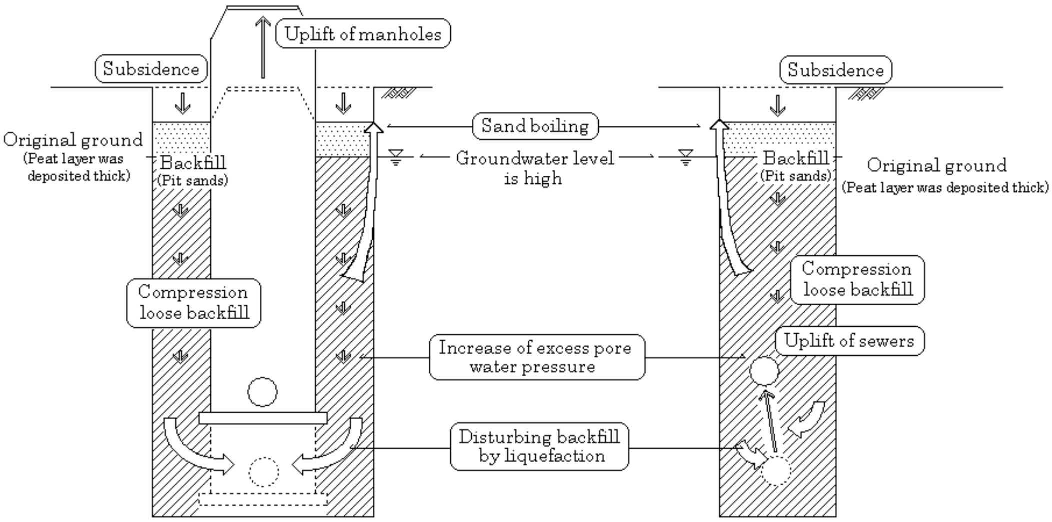

Fig. 14: Mechanisms of typical damage due to liquefaction [6]

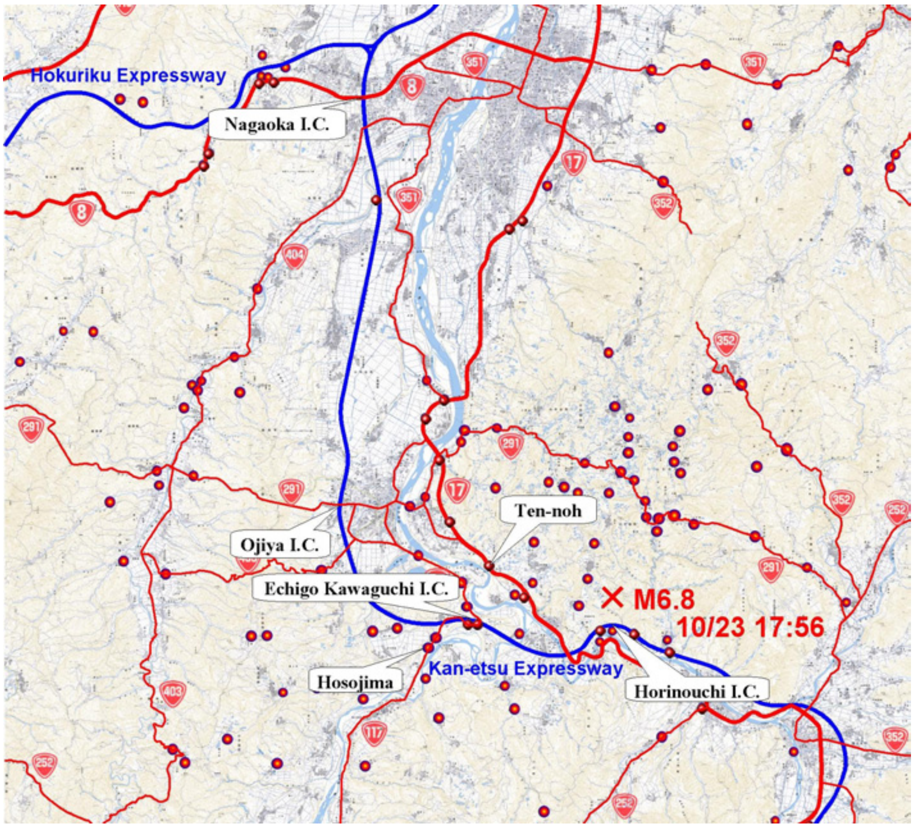

Fig. 15: Distribution of damaged earthworks

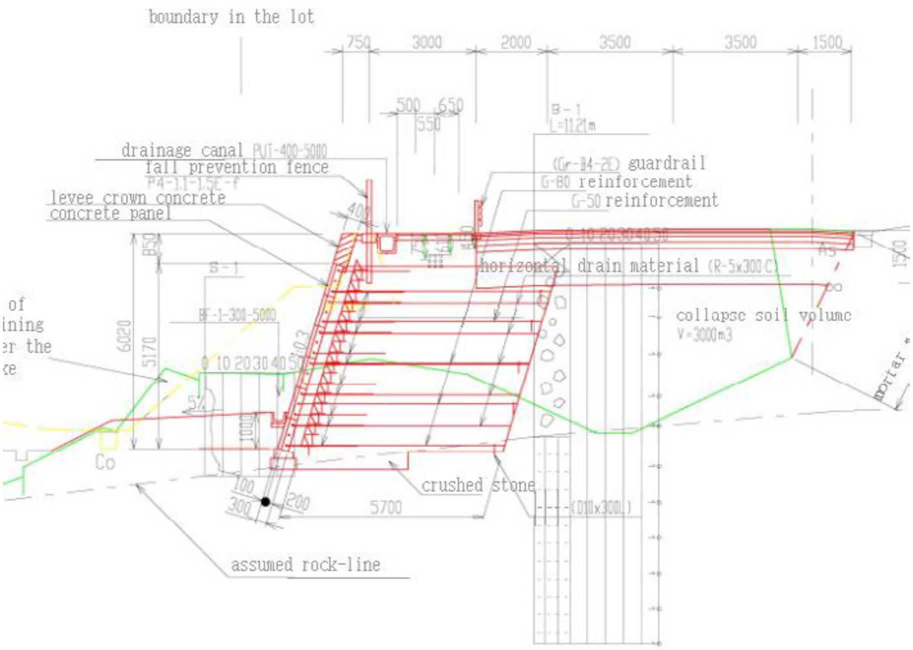

Fig. 16: Cross section of restoration work at Ten-noh in National Road No.17

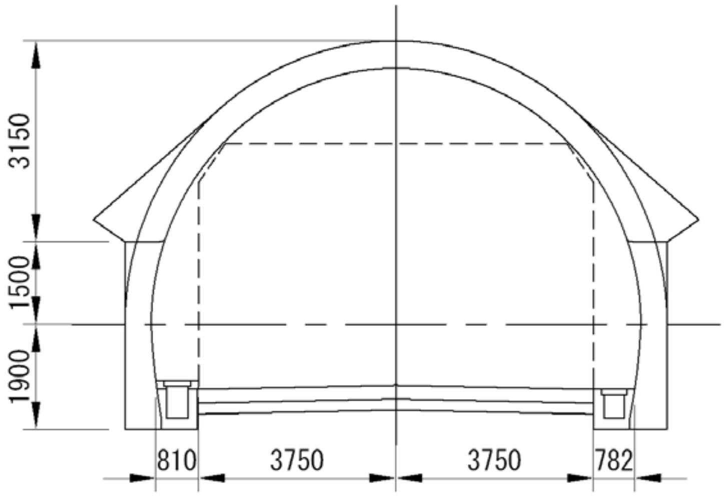

Fig. 17: Cross section of Wanatsu Tunnel (Unit: mm)

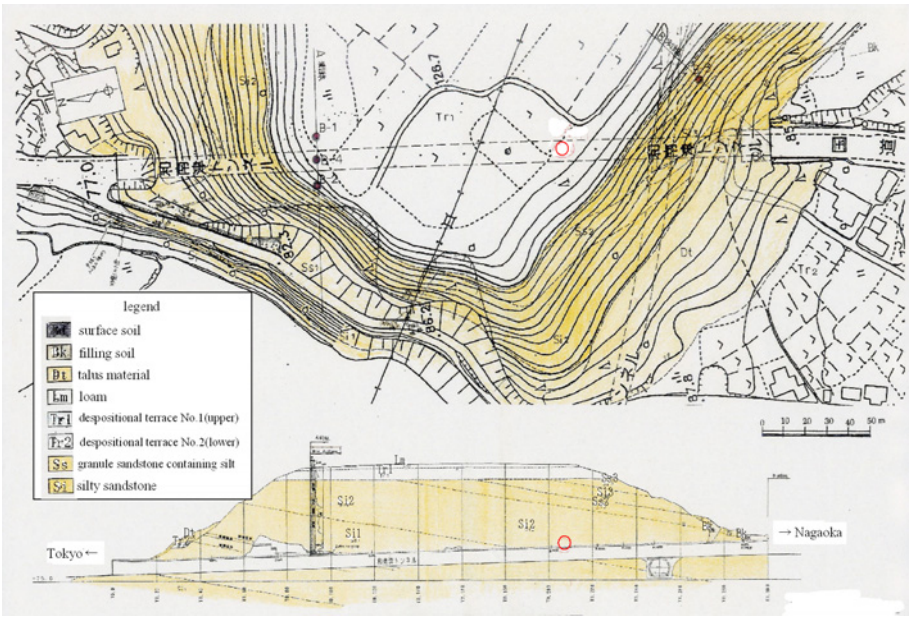

Fig. 18: Plan view and longitudinal section of Wanatsu Tunnel with geological formation

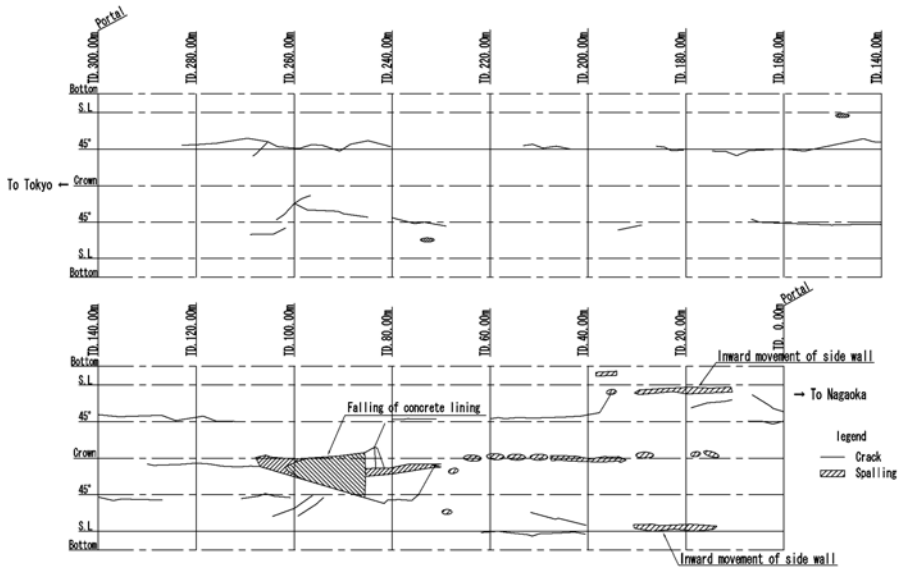

Fig. 19: Locations of crack in tunnel lining on tunnel expansion plan

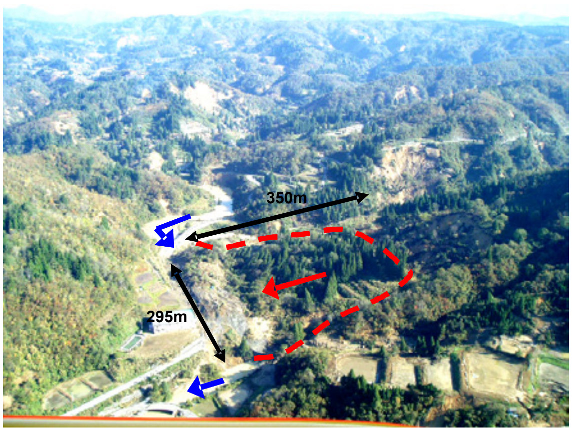

Photo 1: Landslide at Higashi-Takezawa

Photo 3: Settlement of road pavement

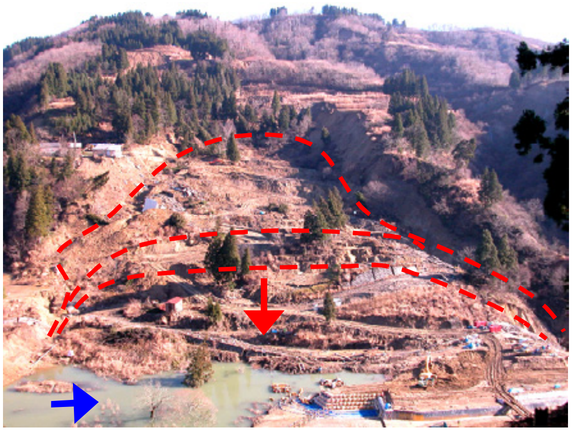

Photo 2: Landslide at Terano

Photo 4: Uplifted manhole

Photo 5: Damaged RC pier in Shinkumi overpass

Photo 6: Failure of side block for shoe in Ojiya Bridge

Photo 7: Sliding failure of embankment slope at 215.1kp in Kan-etsu Expressway

Photo 8: Sliding failure of embankment slope at Hosojima in National Road No.117

Photo 9: Sliding failure at Ten-noh in National Road No.17

Photo 10: Aerial picture of sliding failure at Ten-noh in National Road No.17

Photo 11: Differential settlement due to underpassing box culvert in Kan-etsu Expressway (near Ojiya IC)

Photo 12: Opening of box culvert (near Ojiya IC)

Photo 13: Damaged L-shaped concrete retaining walls supporting toe of road embankment of Kan-etsu expressway

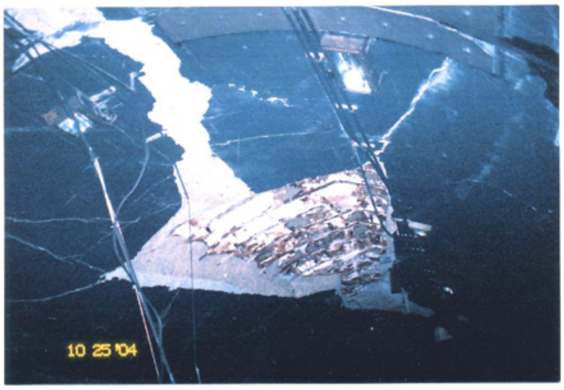

Photo 14: Large mass of concrete lining fell off from the tunnel crown

Photo 15: Deformation of lateral groove